2017 14th International Conference on Ubiquitous Robots and Ambient Intelligence (URAI)
June 28 - July 1, 2017 at Maison Glad Jeju, Jeju, Korea

Modeling and Control of Quadrotor UAV Subject to Variations in Center of Gravity and Mass

Sangheon Lee, Dipak Kumar Giri and Hungsun Son
Department of Mechanical and Nuclear Engineering, UNIST, Ulsan, Korea
(E-mails: ssle8653@unist.ac.kr,judipakkumar@gmail.com, hson@unist.ac.kr)

Abstract – Variations of a center of gravity (COG) and mass make difficulties for control of quadrotors. For example, there are situations such as flight with swing load or with sloshing fuel. These problems leave room for uncertainties in the attitude and position control systems. To mitigate the above-mentioned effects, effective control algorithm must be developed based on modified dynamics of the quadrotors with considering mass and COG variations. The complete mathematical formulations of translation and rotational dynamics of the quadrotor are derived with considering the effect of swing load motion. Hence, the formulations are quite different with the one used in the existing quadrotor dynamics. The proposed model consists of 6-DOF quadrotor dynamics model, and 3-DOF of swing load model. A cascade PD control algorithm is considered for the attitude and position control for such quadrotor. Simulation results indicate that the control algorithm works well in the quadrotor flight with the COG and mass variations.

Keywords – quadrotor, slosh, quadrotor with variation of mass or COG, PD control.

1. Introduction

In the last few decades, with the advancement in the unmanned aerial vehicles and modern control methodologies, the research works for addressing the quadrotor aircrafts with swing load become a popular research subject [1-3]. For the conventional helicopter, the research works with swing load started in the late 60s and the considerable works on modeling and control have received substantial attention [4]. However, there are very few unified works have been done so far for modeling and control of such systems with the consideration of complete mathematical formulations based on the variations in mass or COG due to swing load. When a load is attached to quadrotor system like a pendulum, it produces swing effect and it leads the difficulty in the modeling and controller design due to coupled effects between load and quadrotor system. [5] In addition, the dynamics of load interfere with tracking a trajectory of quadrotor system. Thus, it is necessary to model the complete mathematical formulations with considerations of mass or COG change due to the swing load and design the controller for the same. Certain approaches have been proposed in the existing literatures to solve the problem of control design for the quadrotor aircrafts with swing load. In [5], the authors developed the adaptive control algorithm for the quadrotor with swing load which was considered as a point mass spherical pendulum. In [6], the analytical expression of the external force and torque acting on the helicopter system because of a slung load were derived and an output/input variance constrained controllers were developed. In [7] A quadrotor dynamic model with plane swing load was presented and that enables finding nominal trajectories with both the minimal and large swing loads for dynamically agile motions. In [8], authors considered the dynamic model with 3D swing load and designed a feedforward controller with input shaping to reduce the vibration by the swing load. An Interconnection and Damping Assignment-Passivity Based Control strategy was considered to suppress the vibration caused by the swing payload; however, the authors were considered the control law for 2D swing load for simplifying the problem [9].

It is observed from these kinds of literature that the dynamics model of the quadrotor system with swing load was developed based on the change of COG by swing motion only. But the case when there is a sloshing load with varying mass received less attention. Also, some researchers developed the dynamic model for plane swing motion only. However, it is not reasonable to consider sloshing motion with mass variation in the practical case of fuel usage or agricultural drones which use pesticide. Aiming at considering the above situations, in this paper, a dynamic model of the quadrotor system is developed with considering an effect due to a mass change rate. In addition, 3D swing motion is considered for deriving the dynamics and cascade PD control algorithm is used for the practical purposes.

This paper is organized as follows: Section 2 represents the dynamic modeling of the quadrotor with sloshing load. Section 3 describes the cascade PD control for the both the position and attitude controls of the proposed system. Section 4 represents the results with no load, with load, and load with mass variation, and Section 4 gives the concluding remark of the paper.

2. State Space Representation of the Dynamic Model of the System

The equation of motion of the quadrotor is derived based on two frames of reference; the Earth-centered reference frame [E] (XYZ) which is fixed on the Earth and body frame $(x_b y_b z_b)$ whose origin coincides at the center of mass of the quadrotors and the axes are aligned along the principle moments of inertia. The position of the quadrotor in the inertial reference frame is denoted by the vector (x, y, z) and the orientation of quadrotor that referred to as roll, pitch and yaw $(\emptyset, \theta, \psi)$ which is measured from the

978-1-5090-3056-9/17/$31.00 ©2017 IEEE

inertial frame of reference. The schematic of a quadrotor with coordinate frames is shown in Fig. 1. Here we have considered another reference frame (f) which is fixed with the center of the water tank attached below the quadrotor (point 'O'). It needs to be mentioned that there is no torque acting on frame (f) as it is subject to roll free system (Pivot). As defining that the [E] and [f] are parallel with each other, same rotational matrix is used when the [B] is transformed into [E] and [f]. Also, the frame [f] moves with linear acceleration caused by motion of the body frame.

State vector consists of 18 variables and which is defined as $X=[x,\dot{x},y,\dot{y},z,\dot{z},\phi,\dot{\phi},\theta,\dot{\theta},\psi,\dot{\psi},x_L,\dot{x}_L,y_L,\dot{y}_L,z_L,\dot{z}_L]$. Here, x_L, y_L, z_L are position of COG of the load in the [f] frame.

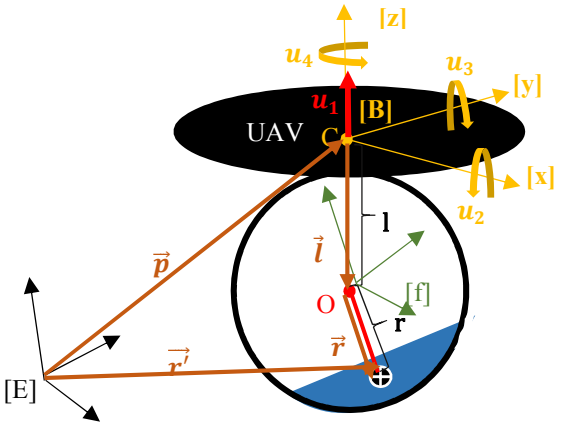

Fig 1. Free body diagram of UAV with sloshing

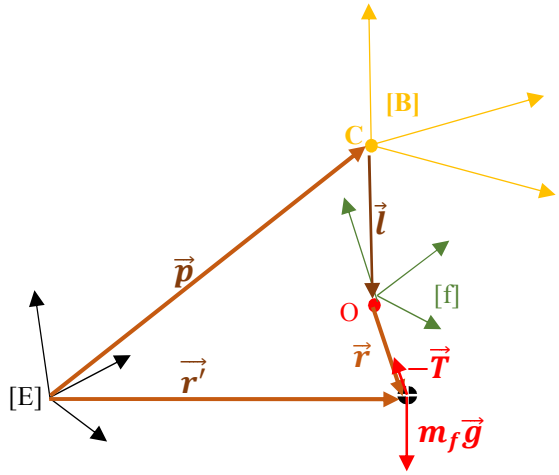

Fig2. Free body diagram of pendulum

The transformation matrix R which transform the frame [B] into the [E] is the product of series of rotation matrices.

$$R = R_{zyx} = R_z \cdot R_y \cdot R_x$$

$$= \begin{bmatrix} c\psi c\theta & c\psi s\phi s\theta - c\phi s\psi & s\phi s\psi + c\phi c\psi s\theta \\ c\theta s\psi & c\phi c\psi + s\phi s\psi s\theta & c\phi s\psi s\theta - c\psi s\phi \\ -s\theta & c\theta s\phi & c\phi c\theta \end{bmatrix}$$

$$= \begin{bmatrix} R_{11}(\eta) & R_{12}(\eta) & R_{13}(\eta) \\ R_{21}(\eta) & R_{22}(\eta) & R_{23}(\eta) \\ R_{31}(\eta) & R_{32}(\eta) & R_{33}(\eta) \end{bmatrix} \quad (1)$$

There are three governing equations of motion (Eqs. (2) - (4)) which is derived based on Newton's 2nd law. The first equation is for translational motion of quadrotor, the second equation is rotational motion of quadrotor and the last one is translational motion of the pendulum (Sloshing dynamics).

$$\ddot{\vec{p}}_E = \begin{bmatrix} \ddot{x} \\ \ddot{y} \\ \ddot{z} \end{bmatrix}_E = \vec{g}_E + \frac{1}{m}\vec{T}_f + \frac{1}{m}R\begin{bmatrix} 0 \\ 0 \\ u_1 \end{bmatrix} \quad (2)$$

$$\ddot{\eta} = [I]\begin{bmatrix} u_2 \\ u_3 \\ u_4 \end{bmatrix} + \vec{l} \times \vec{T}_B \quad (3)$$

$$\frac{d\vec{L}}{dt} = -\vec{T}_f + m_L \vec{g}_E \quad (4)$$

where η is the attitude of the quadrotor, [I] is the moment of inertia matrix of the quadrotor, u_1 is the total thrust, u_2, u_3, u_4 are roll, pitch and yaw moments; $\vec{L}$ is the linear momentum of the pendulum; m and m_L are the mass of the quadrotor and the load, respectively. Let $\vec{T}$ be the tension of the chord (Fig 2). The tension $\vec{T}_f$ is represented in the frame [f] and $\vec{T}_b$ is represented in the frame [B]

The tension of the chord is the inner force of the system, so the tension is determined by the states of the system. The linear density of tension (T) of the pendulum chord is obtained as

$$T = f_T(X) + g_T(X)u_1 \quad (5)$$

where $f_T(x)$ and $g_T(x)$ are obtained as

$$f_T(x) = \frac{m_L m}{(m_L + m)}\left(\frac{v_L^2 - \ddot{r}r - \dot{r}^2}{r^2}\right)$$

$$+\frac{m\dot{m}_L}{(m_L+m)r^2}\left(-x_L(\dot{x}+\dot{x}_L) - y_L(\dot{y}+\dot{y}_L) + (r^2 - z_L^2)(\dot{z}+\dot{z}_L)\right)$$

$$g_T(x) = -\frac{m_L}{(m_L+m)r^2}\left(x_L R_{13}(\eta) + y_L R_{23}(\eta) + z_L R_{33}(\eta)\right)$$

$$\vec{T}_f = (f_T(X) + g_T(X)u_1)\begin{bmatrix} x_L \\ y_L \\ z_L \end{bmatrix}$$

Here, v_L is the speed of the COG of load in the [f] frame and r is the length of the chord. The translational and rotational motion of the quadrotor system are obtained as

$$\begin{bmatrix} \ddot{x} \\ \ddot{y} \\ \ddot{z} \end{bmatrix} = \begin{bmatrix} 0 \\ 0 \\ -g \end{bmatrix} + \frac{1}{m}\left((f_T(x) + g_T(x)u_1)\begin{bmatrix} x_L \\ y_L \\ z_L \end{bmatrix} + \begin{bmatrix} R_{13}(\eta) \\ R_{23}(\eta) \\ R_{33}(\eta) \end{bmatrix} u_1\right) \quad (6)$$

$$\begin{bmatrix}\ddot{\phi}\\ \ddot{\theta}\\ \ddot{\psi}\end{bmatrix}=\begin{bmatrix}f_4(x)\\ f_5(x)\\ 0\end{bmatrix}+\begin{bmatrix}g_4(x) & \frac{1}{I_{xx}} & 0 & 0\\ g_5(x) & 0 & \frac{1}{I_{yy}} & 0\\ 0 & 0 & 0 & \frac{1}{I_{zz}}\end{bmatrix}\begin{bmatrix}u_1\\ u_2\\ u_3\\ u_4\end{bmatrix} \quad (7)$$

where

$$f_4(x)=l(x_L R_{12}(\eta)+y_L R_{22}(\eta)+z_L R_{32}(\eta))f_T(x)$$
$$f_5(x)=l(x_L R_{11}(\eta)+y_L R_{21}(\eta)+z_L R_{31}(\eta))f_T(x)$$
$$g_4(x)=l(x_L R_{12}(\eta)+y_L R_{22}(\eta)+z_L R_{32}(\eta))g_T(x)$$
$$g_5(x)=l(x_L R_{11}(\eta)+y_L R_{21}(\eta)+z_L R_{31}(\eta))g_T(x)$$

where l is the offset between the COG of the quadrotor (C) and the pivot of the pendulum (O). (Fig 1)

The translational motion of the load is obtained as

$$\begin{bmatrix}\ddot{x}_L\\ \ddot{y}_L\\ \ddot{z}_L\end{bmatrix}=\begin{bmatrix}-\frac{(m+m_L)}{m_L m}f_T(x)x_L-\frac{\dot{m}_L}{m_L}(\dot{x}+\dot{x}_L)\\ -\frac{(m+m_L)}{m_L m}f_T(x)y_L-\frac{\dot{m}_L}{m_L}(\dot{y}+\dot{y}_L)\\ -\frac{(m+m_L)}{m_L m}f_T(x)z_L-\frac{\dot{m}_L}{m_L}(\dot{z}+\dot{z}_L)\end{bmatrix} \quad (8)$$
$$+\begin{bmatrix}-\frac{(m+m_L)}{mm_L}g_T(x)x_L-\frac{R_{13}(\eta)}{m}\\ -\frac{(m+m_L)}{mm_L}g_T(x)y_L-\frac{R_{23}(\eta)}{m}\\ -\frac{(m+m_L)}{mm_L}g_T(x)z_L-\frac{R_{33}(\eta)}{m}\end{bmatrix}u_1$$

It can be observed from the above mathematical formulations for the quadrotor system with sloshing that there are in total nine states that required to be controlled. This complicated system can be comprised by three typical groups of equations. Each of them describes subsystem with coupled terms.

3. Control of Quadrotor

A simple PD control is used for attitude and position control of the quadrotor system defined in the above section. The control law designed in this paper without considering the sloshing model of the load as it is very difficult to take sloshing dynamic into account for designing control law. The overall control structure is presented in Fig. 3.

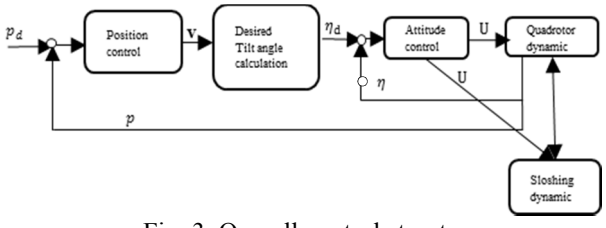

Fig. 3. Overall control structure

Table 1 Control variables

Variable	name
$\boldsymbol{p_d}$ $=(x_d, y_d, z_d)$	Desired Position of quadrotor
$\mathbf{v}=(v_x, v_y, v_z)$	Virtual control output for position control
$\boldsymbol{\eta_d}$ $=(\phi_d, \theta_d, \psi_d)$	Desired Attitude of quadrotor
U	Control output for Quadrotor (Dynamic input)

3.1 Position Control Law

Three virtual controls namely v_x, v_y and v_z are considered for position control (x-, y- and z-), which are equivalent to $\ddot{x}, \ddot{y}$ *and* $\ddot{z}$ (acceleration of translational motion), respectively. In other words, it is desired translational acceleration to reach the desired position of quadrotor. The virtual controls are determined by cascade PD control algorithm consisting of two loops as shown in Fig. 4. In the control structure, the outer loop is for position, and the inner loop is for velocity control.

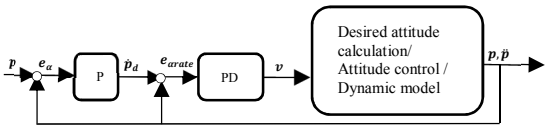

Fig. 4 Position control structure

From the outer loop (P controller), desired velocity is determined.

$$\dot{\alpha}_d = P_\alpha e_\alpha \quad (9)$$

where e_α is

$$e_\alpha = \alpha_d - \alpha \quad (\alpha = x, y \text{ and } z)$$

where $\alpha = x, y$ and z, P_α is the proportional gain in the outer loop (Position control loop). Then using desired velocity, the inner loop PD control algorithm can be designed to produce the virtual controls. The velocity error and virtual controls can be written as

$$e_{\alpha rate} = \dot{\alpha}_d - \dot{\alpha} \quad (10)$$
$$v_\alpha = P_{\alpha rate} e_{\alpha rate} + D_{\alpha rate}\dot{e}_{\alpha rate}$$

where $e_{\alpha rate}$ is the error in translational velocity, $P_{\alpha rate}$ and $D_{\alpha rate}$ are the proportional and derivative gains in the inner loop (velocity control loop). Now, considering dynamic equations of the translational motion of the quadrotor without sloshing, virtual controls can be considered as

$$v_x = (\cos\phi\sin\theta\cos\psi + \sin\psi\sin\phi)\frac{u_1}{m} \quad (11)$$
$$v_y = (\cos\phi\sin\theta\sin\psi - \sin\phi\cos\psi)\frac{u_1}{m}$$
$$v_z = (\cos\phi\cos\theta)\frac{u_1}{m} - g$$

It is possible to consider above equations set as a simultaneous equation about roll (ϕ) ,pitch (θ) angles and u_1. The angles ϕ and θ can be considered for the desired attitude state for satisfying position control law. Hence, these angles can be replaced into desired roll (ϕ_d) and pitch (θ_d), and can be determined as

$$\theta_d = \arctan\left(\frac{v_x \cos\psi + v_y \sin\psi}{v_z + g}\right) \tag{12}$$

$$\phi_d = \arctan\left(\left(\frac{v_x}{v_z + g} - \tan\theta_d \cos\psi\right)\frac{\cos\theta_d}{\sin\psi}\right)$$

Using the desired angles in Eq. (12), the desired control u_1 for position control can be determined as

$$u_1 = m \cdot \frac{u_z + g}{\cos\phi_d \cos\theta_d} \tag{13}$$

3.2 Attitude Control Law

Like position control, the same PD control algorithm can be considered for the attitude control. The block diagram of the attitude control loop is shown in Fig. 5. It consists of outer loop for attitude control and inner loop for attitude rate control. Errors in attitude and attitude rate can be used to obtain roll, pitch, and yaw moment as below

$$e_\beta = \beta_d - \beta \tag{14}$$

$$\dot{\beta}_d = P_\beta e_\beta$$

$$e_{(\beta)rate} = \dot{\beta}_d - \beta \tag{15}$$

$$u_i = P_{\beta rate} e_{\beta rate} + D_{\beta rate} \dot{e}_{\beta rate}$$

where $i = 2,3$ and 4 corresponding to $\beta = \emptyset, \theta$ and ψ, e_β is the attitude error and $e_{\beta rate}$ is the attitude rate error. P_β is the proportional gain in the outer loop (Attitude control), $P_{\beta rate}$ and $D_{\beta rate}$ are the proportional and derivative gains in the inner loop (Attitude rate control).

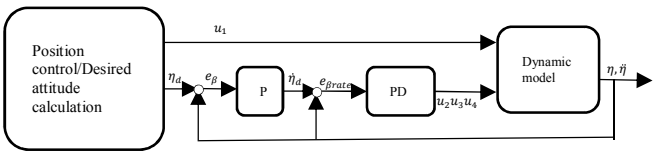

Fig. 5 Attitude control structure

4. Results and Discussions

To show the efficacy of the proposed system, three simulations are considered. In each of the simulations, the magnitude of the thrust level of each motor are is set to half of quadrotor mass

Following three simulations are carried out with different load mass and mass loss rate: constant 3kg load in the first simulation and constant 0.5kg in the second. Lastly -0.05kg/s mass loss rate with 3kg initial load mass. The value of quadrotor parameters is set as $\mathrm{m} = 6.5\mathrm{kg}, I_{xx} = I_{yy} = 0.18, I_{zz} = 0.35, l = 0.1m$. And initial length of the chord (r_0) depends on initial load mass $(m_{L,0})$. In the first and third simulations, r_0 is $0.05m$. And in the second simulation it is 0.0917m.

Every initial state is chosen as zero in all simulations. And desired setpoint x, y and z increase by 1m every 8s, respectively. And desired yaw is commanded as 0.1. The control gains for all the simulations are shown in Table 2. And all simulation is conducted by Runge-Kutta 4 method.

Table 2. PID gain set for control simulation

Gain	Value	Gain	Value	Gain	Value
P_x P_y	3.838	P_{xrate} P_{yrate}	4	D_{xrate} D_{yrate}	2
P_z	3.838	P_{zrate}	108.55	D_{zrate}	0.001
P_ϕ P_θ	11.78	$P_{\phi rate}$ $P_{\theta rate}$	19.44	$D_{\phi rate}$ $D_{\theta rate}$	0.0194
P_ψ	11.78	$P_{\psi rate}$	37.8	$D_{\psi rate}$	0.0378

The first simulation is carried out for relatively heavy(3kg) swing load mass. It can be observed from Figs. 6 to 8.

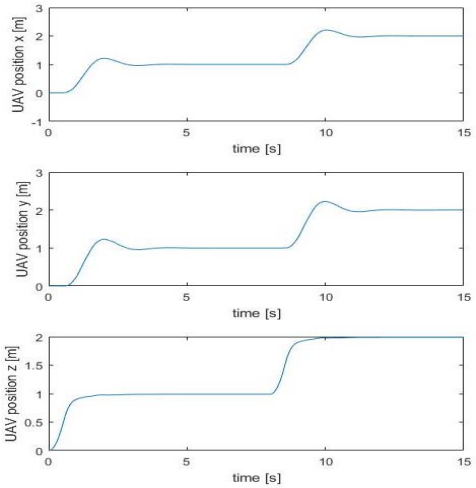

Fig. 6: Position of UAV with 3kg load

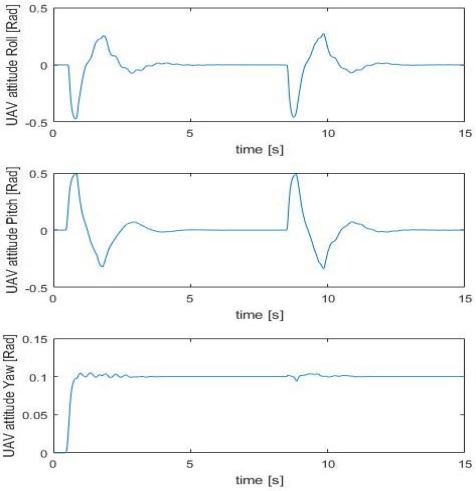

Fig. 7: Attitude of UAV with 3kg load

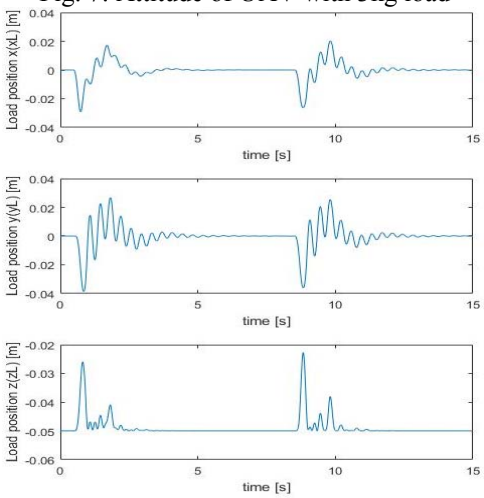

Fig. 8: Position of 3kg load

Even though there is sloshing in the load, UAV position goes to setpoint stably. Furthermore, UAV attitude goes to zero with less swing

The second simulation is carried out with relatively light (0.5 kg) swing load. It can be observed from Figs. 9 to 11. In this simulation, UAV position converges to the setpoint stably, like first simulation. However, because of little inertia of the load, sloshing of the load is severe. It causes fluctuation in the UAV attitude.

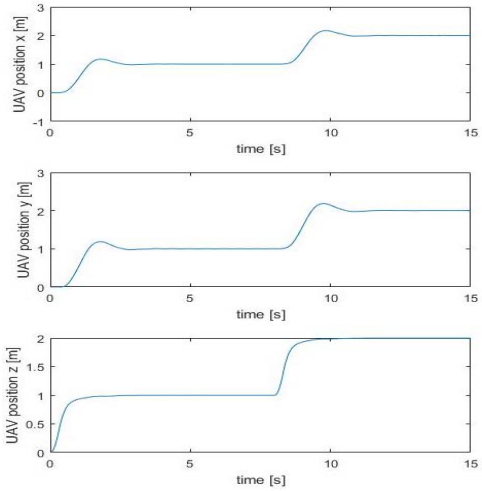

Fig. 9: Position of UAV with 0.5kg load

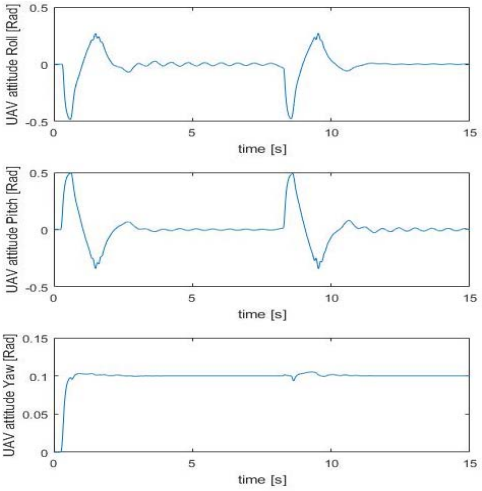

Fig. 10: Attitude of UAV with 0.5kg load

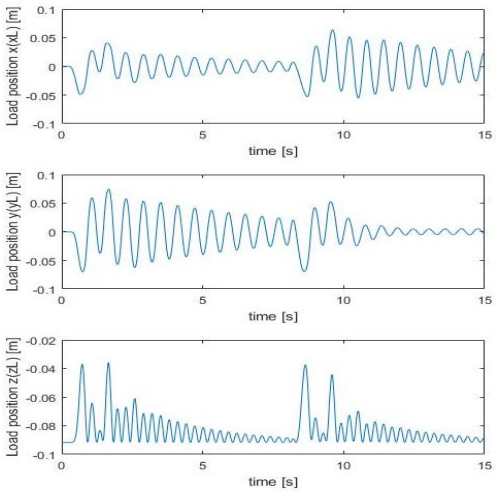

Fig. 11: Position of 0.5kg load

In third simulation, it is carried out for varying mass load. As mentioned before, load conditions are taken as $\dot{m}_L = -0.05\text{kg/s}$ with $m_{L,0} = 3kg$ and $r_0 = 0.05m$. As load mass decreasing, length of the pendulum chord increases. In this example, the fuel tank is assumed to be circular cylinder, which indicates if the $\dot{m}_L$ is constant, the $\dot{r}$ becomes constant; In the simulation, $\dot{r} = 0.01\text{m/s}$. And it means $\ddot{r} = 0$. Plots of this example are shown in Figs. 12 to 14.

The convergence of position and attitude of UAV is achieved even for the different system properties. It can be observed from Fig. 14 that the vertical length of the chord increases. This is due to the fact of decreasing mass. Also, the more load mass decreases, the severer sloshing occurs (Fig 14). And It causes a fluctuation of UAV attitude (Fig 13). This is because UAV attitude dynamic and sloshing dynamic is coupled.

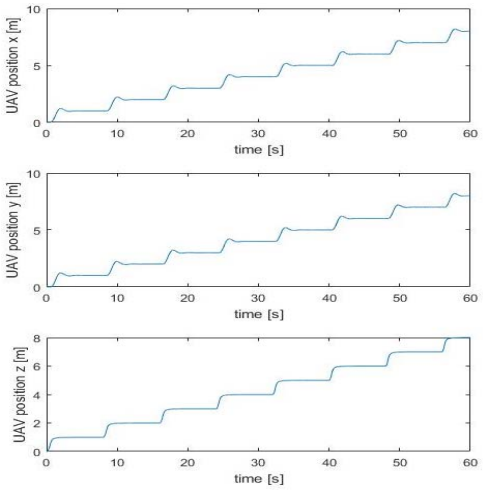

Fig.12: Position of UAV with sloshing and mass variation

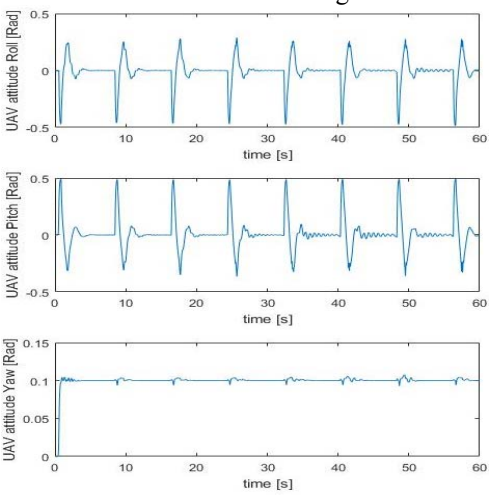

Fig.13: Attitude of UAV with sloshing and mass variation

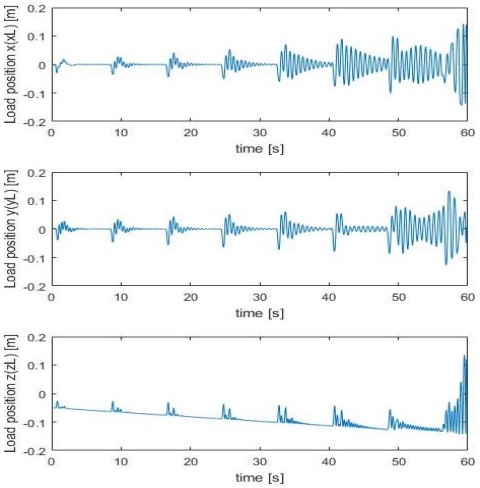

Fig.14: Position of mass varying load

The same control gains are used throughout all the simulations. The control gains, used in the first example which is for constant 3kg load case, can also make the others stable. However, comparing the others with first simulation, there are the oscillations in attitude because of stronger sloshing effect. Especially, in third simulation, the oscillations in attitude changes as the inertia of the load changes with time. Therefore, for achieving better control performance, it is critical to consider the change of system properties and the sloshing effect when designing a new control law.

3. Conclusion

In this paper, the position and attitude control of a quadrotor UAV with variations in mass and COG due to swing load were presented. The swing load is hooked by a cable from the quadrotor and behave like a pendulum. The mathematical formulations of the quadrotor dynamics together with sloshing dynamics were developed. The equations of external force and torque caused by the swing load were derived. A simple PD control algorithm was used for the control purposes. It was observed that the PD control works very well for the cases with heavy load and light load. Also, when there was a change in mass in the load, the system is stable with the designed PD control. Furthermore, it can be concluded that by changing the load mass, the effect of sloshing changes too. Therefore, it is necessary to develop adaptive control for varying system or control law for reducing the sloshing effect. Also, as future works, it is important to think about observer to estimate the position of the load. In addition, through stability analysis and experimental results, the effect of sloshing on the UAV and performance of control should be verified.

Acknowledgement

This work was supported by Research of Advanced Technology for Radiation Monitoring in Case of Emergency (2.160440.01) of Korea Institute of Nuclear Safety and the 2017 Research Fund (1.170013.01 and 1.170006.01) of UNIST(Ulsan National Institute of Science and Technology).

References

[1] W. MacKunis, Z. D. Wilcox, M. K. Kaiser, W.E. Dixon, "Global adaptive output feedback tracking control of an unmanned aerial vehicle." IEEE Transactions on Control Systems Technology, Vol. 18, No. 6, pp. 1390-1397, 2010.

[2] R. Mahony, V.Kumar, and P. Corke, "Multirotor aerial vehicles: modeling, estimation, and control of quadrotor." IEEE Robotics and Automation Magazine, vol. 19, no. 3, pp. 20-32, 2012.

[3] L. Marconi, R. Naldi, L. Gentili, "Modelling and control of a flying robot interacting with the environment." Automatica, vol. 47, no. pp. 2571-2583, 2011.

[4] T.A. Dukes, "Maneuvering heavy sling loads near hover, Part II: Some elementary maneuvers." Journal of the American Helicopter Society, vol. 18, no. 3, DOI: 10.4050/JAHS.18.17, 1973.

[5] Y. Feng, et.al., "Adaptive Controller Design for Generic Quadrotor Aircraft Platform Subject to Slung Load," Proc. of the IEEE 28th Candaian Conf. on Elect. And Comp. Halifax, Canada, pp. 1135-1139, 2015.

[6] T. Oktay, C.l Sultan," Modeling and control of a helicopter slung-load system." Aerospace Science and Technology, vol. 29, no. 1, pp.206- 222, 2013.

[7] K. Sreenath, N. Michael, and V. Kumar, "Trajectory generation and control of a quadrotor with a cable-suspended load – a differently-flat hybrid system," IEEE Int. Conf. on Robotics and Automation, Karlsuhe, Germany, pp. 4888-4895.

[8] S. Sadr, S. Ali, A. Moosavian, P. Zarafshan, "Dynamics Modeling and Control of a Quadrotor with Swing Load," Journal of Robotics, Vol. 2014, ID. 265897, 2014.

[9] M. E. Guerrero, D. A. Mercado, R. Lozano, and C. D. Garcia, "Passivity based control for a quadrotor UAV transporting a Cable-Suspended Payload with Minimum Swing," IEEE 54th Annual Conference on Decision and Control, Osaka, Japan, pp. 6718-6723, 2015.